Appears in ASME Journal of Computational and Nonlinear Dynamics 1(4): 358-367, Oct 2006.

OPTIMAL INPUTS FOR PHASE MODELS OF SPIKING NEURONS

Jeff Moehlis
Dept. of Mechanical Engineering
University of California, Santa Barbara
Santa Barbara, CA 93106
Email: moehlis@engineering.ucsb.edu

Eric Shea-Brown
Courant Inst. for Mathematical Sciences
and Center for Neural Science
New York University
New York, NY 10012
Email: ebrown@math.nyu.edu

Herschel Rabitz
Dept. of Chemistry
Princeton University
Princeton, NJ 08544
Email: hrabitz@princeton.edu

ABSTRACT

Variational methods are used to determine the optimal currents that elicit spikes in various phase reductions of neural oscillator models. We show that, for a given reduced neuron model and target spike time, there is a unique current that minimizes a square-integral measure of its amplitude. For intrinsically oscillatory models, we further demonstrate that the form and scaling of this current is determined by the model's phase response curve. These results reflect the role of intrinsic neural dynamics in determining the time course of synaptic inputs to which a neuron is optimally tuned to respond, and are illustrated using phase reductions of neural models valid near typical bifurcations to periodic firing, as well as the Hodgkin-Huxley equations.

1 Introduction

Phase-reduced models of neurons have traditionally been used to investigate either the patterns of synchrony that result from the type and architecture of coupling [2,3,7,12–14,17,22], or the response of large groups of oscillators to external stimuli [4,5,21]. In all of these cases, the inputs to the model cells were fixed by model definition at the outset, and the dynamics of phase models of networks or populations were analyzed in detail. The present article takes a complementary, control-theoretic approach that is related to probabilistic 'spike-triggered' methods [19]: we fix at the outset a feature of the dynamical trajectories of interest – spiking at a precise time t_1 – and study the neural inputs that lead to this outcome. By computing the optimal such input, according to a measure of the input strength required to elicit the spike, we identify the signal which the neuron is optimally 'tuned' to respond to. We view the present work as part of the first attempts [11,23] to understand the dynamical response of neurons using control theory, and hope that insights from this general perspective will ultimately be combined with the 'forward' dynamics results mentioned above to enhance our understanding of neural processing.

2 Optimal Current for Specified Time of Firing

2.1 Problem formulation

Consider the phase model for a spiking (i.e., firing) neuron

$$\frac{d\theta}{dt} = f(\theta) + Z(\theta)I(t), \tag{2.1}$$

where $f(\theta)$ gives the neuron's baseline dynamics, $Z(\theta)$ is its phase sensitivity function, and $I(t)$ is a current stimulus (e.g., [4, 24]). We assume that $Z(\theta)$ vanishes only at isolated points, and that $f(\theta) > 0$ at these points, so orbits of full revolution are possible. Here θ is 2π-periodic on $[0, 2\pi)$, and by convention $\theta = 0$ corresponds to the spiking of the neuron.

Suppose that, for a specified time t_1, for all stimuli $I(t)$ which evolve $\theta(t)$ via (2.1) from $\theta(0) = 0$ to $\theta(t_1) = 2\pi$ (that is, which cause the cell to spike at time t_1, following a spike at time 0), we want to find the one which minimizes the cost function $G[I(t)] = \int_0^{t_1} [I(t)]^2 dt$, the square-integral cost on the current. Other choices, including costs on the time derivative of the current, lead to alternate equations below, but can be handled similarly (cf. [6]).

We apply calculus of variations to minimize [11]

$$C[I(t)] = \int_0^{t_1} \underbrace{\left\{ [I(t)]^2 + \lambda \left(\frac{d\theta}{dt} - f(\theta) - Z(\theta) I(t) \right) \right\}}_{P[I(t)]} dt, \quad (2.2)$$

with λ being the Lagrange multiplier associated with requiring that the dynamics satisfy (2.1). The associated Euler-Lagrange equations are

$$\frac{\partial P}{\partial I} = \frac{d}{dt}\left(\frac{\partial P}{\partial \dot{I}}\right), \qquad \frac{\partial P}{\partial \theta} = \frac{d}{dt}\left(\frac{\partial P}{\partial \dot{\theta}}\right), \qquad \frac{\partial P}{\partial \lambda} = \frac{d}{dt}\left(\frac{\partial P}{\partial \dot{\lambda}}\right),$$

giving

$$I(t) = \frac{\lambda(t) Z(\theta(t))}{2}, \quad (2.3)$$

$$\frac{d\theta}{dt} = f(\theta) + Z(\theta) I(t) = f(\theta) + \frac{\lambda [Z(\theta)]^2}{2}, \quad (2.4)$$

$$\frac{d\lambda}{dt} = -\lambda f'(\theta) - \lambda Z'(\theta) I(t) = -\lambda f'(\theta) - \frac{\lambda^2 Z(\theta) Z'(\theta)}{2}. \quad (2.5)$$

To find the optimal $I(t)$, (2.4) and (2.5) need to be solved subject to the conditions $\theta(0) = 0, \theta(t_1) = 2\pi$. This requires that we find the appropriate initial condition $\lambda(0) \equiv \lambda_0$, which can be done with appropriate numerical methods. The solution $(\theta(t), \lambda(t))$ using this initial condition can then be used in (2.3) to give the optimal stimulus $I(t)$. (For higher dimensional neural models, such as the Hodgkin-Huxley equations considered below, gradient-based numerical models that iteratively update $I(t)$ via the variational derivative $\frac{\delta P}{\delta I(t)}$ may be required; see [6].)

We observe that the Hamiltonian $H(\theta, \lambda) = \lambda f(\theta) + \frac{1}{4}\lambda^2 [Z(\theta)]^2$ is conserved on trajectories for the Euler-Lagrange equations (2.4) and (2.5). Taking initial conditions $(\theta, \lambda) = (0, \lambda_0)$ with $H_0 \equiv H(0, \lambda_0)$, the trajectories thus satisfy

$$\frac{1}{4}\lambda^2 [Z(\theta)]^2 + \lambda f(\theta) - H_0 = 0. \quad (2.6)$$

2.2 Existence and uniqueness of optimal inputs $I(t)$

As mentioned above, the trajectories of interest are orbits which go from $\theta = 0$ to $\theta = 2\pi$ over the timespan $[0, t_1]$. We now show that there is a unique such orbit, and hence input $I(t)$, that is optimal in the sense introduced in the previous section. We refer to this orbit as the *optimal trajectory*.

First, we introduce two assumptions

$$Z(0) = 0, \qquad f(0) > 0. \quad (2.7)$$

That is, we assume that the phase sensitivity function $Z(\cdot)$ vanishes at the spike phase $\theta = 0$ and that the intrinsic phase dynamics are increasing at this point. These conditions are required for well-defined phase reductions of spiking neurons [4], as they ensure that the spike phase is not crossed 'backwards.'

Lemma 2.1 *Assume that* (2.7) *holds. Then* $\frac{d\theta}{dt} > 0$ *for all* $t \in [0, t_1]$ *for the optimal trajectory.*

Proof. Consider a candidate optimal trajectory $\{(\theta(t), \lambda(t))\}$, $0 \le t \le t_1$ which solves (2.4)-(2.5). From (2.7), we have $\frac{d\theta}{dt}|_{t=0} > 0$. Assume in point of contradiction that there exists a time $0 < \hat{t} < t_1$ such that $\frac{d\theta}{dt}|_{t=\hat{t}} < 0$. Since $\theta(t_1) = 2\pi$, in this case there also exists a phase $\bar{\theta} < 2\pi$ such that $\theta(t) = \bar{\theta}$ for three distinct times between 0 and t_1. A quick sketch in the (θ, λ) plane shows that, since any trajectory $\{(\theta(t), \lambda(t))\}$ is not self-intersecting, the trajectory under our assumption contains three distinct points $(\bar{\theta}, \lambda_j)$, $j = 1, 2, 3$. However, the trajectory must also be a level set of the Hamiltonian; from Eqn. (2.6), which is quadratic in $\lambda(\theta)$, such a level set contains at most two points $(\theta, \lambda(\theta))$ for any value of θ. Therefore, a contradiction has been reached, and the lemma follows. □

Lemma 2.2 *Assume that* (2.7) *holds. For an optimal solution,*

$$\lambda(\theta)[Z(\theta)]^2 = 2\left[-f(\theta) + \sqrt{[f(\theta)]^2 + [Z(\theta)]^2 H_0} \right]. \quad (2.8)$$

Proof. Multiplying (2.6) by $[Z(\theta)]^2$ and solving the resulting quadratic equation in $\lambda(\theta)[Z(\theta)]^2$ gives

$$\lambda(\theta)[Z(\theta)]^2 = 2\left[-f(\theta) \pm \sqrt{[f(\theta)]^2 + [Z(\theta)]^2 H_0} \right].$$

However, (2.4) shows that $\frac{d\theta}{dt} < 0$ whenever $\lambda(\theta)[Z(\theta)]^2/2 < -f(\theta)$. Therefore, from Lemma 2.1, we see that optimal solutions only follow the '+' branch. □

Now, we give the main result of this section:

Proposition 2.3 *Assume that* (2.7) *holds. Then for any* $t_1 > 0$, *an optimal trajectory exists and is unique.*

Proof. Due to Lemma 2.1, we may rewrite (2.4) as follows:

$$t_1 = \int_0^{t_1} dt = \int_0^{2\pi} \frac{d\theta}{f(\theta) + \frac{\lambda [Z(\theta)]^2}{2}}, \quad (2.9)$$

Substituting from Lemma 2.2 then gives

$$t_1 = \int_0^{2\pi} \frac{d\theta}{\sqrt{[f(\theta)]^2 + [Z(\theta)]^2 H_0}}, \quad . \tag{2.10}$$

Differentiating, we have

$$\frac{\partial t_1}{\partial H_0} = -\frac{1}{2}\int_0^{2\pi} \frac{[Z(\theta)]^2 d\theta}{([f(\theta)]^2 + [Z(\theta)]^2 H_0)^{3/2}} < 0, \tag{2.11}$$

provided $[f(\theta)]^2 + [Z(\theta)]^2 H_0 > 0$, which is necessary for (2.8) to give a valid trajectory. Thus, t_1 decreases monotonically as H_0 increases. Noting that λ_0 varies monotonically with H_0 under our assumptions (2.7) (in fact, $H_0 = f(0)\lambda_0$), we conclude that there is at most one value of λ_0 which gives a trajectory with a particular t_1. Examining (2.10) and recalling our assumption from the outset that $Z(\theta)$ vanishes only at isolated points, and that $f(\theta) > 0$ at these points, we see that (i) by choosing H_0 (and hence λ_0) to be arbitrarily large, an optimal trajectory with arbitrarily small t_1 may be found; (ii) by choosing H_0 to approach $\sup_\theta \left(-[f(\theta)]^2/[Z(\theta)]^2\right)$ from above, an optimal trajectory with arbitrarily large t_1 may be found. □

2.3 Intrinsically oscillatory neurons

For the special case that $f(\theta) = \omega$ = constant, so that the neuron fires periodically with period $T = 2\pi/\omega$ in the absence of input $I(t)$, $Z(\theta)$ is called the phase response curve (PRC). Then (2.4)-(2.5) have fixed points (θ_f, λ_f) that satisfy $Z'(\theta_f) = 0, \lambda_f = -2\omega/[Z(\theta_f)]^2$. The eigenvalues of the Jacobian evaluated at these fixed points are $\pm\omega\sqrt{-Z''(\theta_f)/Z(\theta_f)}$. If $Z''(\theta_f)$ and $Z(\theta_f)$ have opposite signs, such a fixed point is a saddle point. The associated stable and unstable manifolds are found to be trajectories with

$$H_0 = H(\theta_f, \lambda_f) = -\omega^2/[Z(\theta_f)]^2. \tag{2.12}$$

Form of optimal current for small $|t_1 - T|$

Suppose $f(\theta) = \omega > 0, Z(0) = 0$, and that the desired spike time t_1 is close to the natural period T. We can then solve (2.4)-(2.5) to lowest order in $|t_1 - T|$ explicitly, demonstrating that in this case the optimal current is proportional to the PRC. Thus, the PRC determines the inputs that neurons are naturally tuned to, in the sense of the optimization problem at hand.

First notice that the line $\lambda = 0$ is invariant for (2.4)-(2.5), and corresponds to $\frac{d\theta}{dt} = \omega$, and hence to $t_1 = T$. From Eqn. (2.3), we see that $I(t) = 0$ in this case; this is expected, as no control is required for an intrinsically oscillatory neuron to fire a spike at its natural period. For $t_1 \approx T$, we Taylor expand t_1 with respect to the initial condition $\lambda(0)$ to give $t_1 = T + \left(\frac{\partial t_1}{\partial \lambda(0)}|_{\lambda(0)=0}\right)\lambda(0)$ to lowest order in $(t_1 - T)$. Thus the initial λ value needed to give a trajectory which reaches $\theta = 2\pi$ at time t_1 is $\lambda(0) \approx (t_1 - T)/\left.\frac{\partial t_1}{\partial \lambda(0)}\right|_{\lambda(0)=0}$, to lowest order in $t_1 - T$. From (2.11), noting for $Z(0) = 0$ that $\lambda(0) = H_0/\omega$, we then have

$$\lambda(0) = -(t_1 - T)2\omega^2 / \int_0^{2\pi} [Z(\theta)]^2 d\theta. \tag{2.13}$$

Letting $t_1 - T = O(\varepsilon)$, and expanding

$$\lambda(t) = \lambda^{(0)}(t) + \varepsilon\lambda^{(1)}(t) + \varepsilon^2\lambda^{(2)}(t) + \cdots \tag{2.14}$$

$$\theta(t) = \theta^{(0)}(t) + \varepsilon\theta^{(1)}(t) + \varepsilon^2\theta^{(2)}(t) + \cdots, \tag{2.15}$$

we find from Eqns. (2.4-2.5) that $\lambda^{(0)} = 0$ and $\lambda^{(1)}(t) = \lambda(0) =$ constant. Furthermore, $\theta^{(0)} = \omega t$. Therefore, from (2.3), the optimal current is given by

$$I(t) = \frac{1}{2}\lambda(0)Z(\theta^{(0)}) + O((t_1 - T)^2) \tag{2.16}$$

$$= -\frac{(t_1 - T)\omega^2 Z(\omega t)}{\int_0^{2\pi}[Z(\theta)]^2 d\theta} + O((t_1 - T)^2). \tag{2.17}$$

Finally, we note that it is expected that since $Z(0) = Z(2\pi) = 0$, the optimal current should vanish for $\theta = 0$ (at $t = 0$) and $\theta = 2\pi$ (at $t = t_1$). This is not the case for (2.17). However, letting $Z(\omega t) \to Z(\omega t - 2\pi t(t_1 - T)/(t_1 T))$, which changes only the $O((t_1 - T)^2)$ terms in (2.17), we obtain an approximation which satisfies these conditions. With this in mind, to lowest order in $t_1 - T$, we approximate the optimal current that causes the neuron to spike at $t_1 \approx T$ as

$$I(t) = -\frac{(t_1 - T)\omega^2 Z(\omega t - 2\pi t(t_1 - T)/(t_1 T))}{\int_0^{2\pi}[Z(\theta)]^2 d\theta} + O((t_1 - T)^2). \tag{2.18}$$

Scaling of optimal current for small $|t_1 - T|$

In [4], it is shown how PRCs for phase reductions of neural oscillators near common bifurcations to periodic firing scale with the baseline firing frequency ω. These reductions have the form $Z(\theta) = Z_d(\omega)\tilde{Z}(\theta)$, where the coefficient $Z_d(\omega)$ captures the scaling with ω. For example, for neurons near a saddle node on a periodic orbit (SNIPER) bifurcation, $Z(\theta) = \frac{c}{\omega}(1 - \cos(\theta))$ [cf. [8]], where c is a model-dependent constant, so $Z_d(\omega) = 1/\omega$; for neurons near a supercritical Hopf transition, $Z(\theta) = \frac{c}{\sqrt{\omega - \omega_H}}\sin(\theta)$ [cf. [10]], where ω_H is the frequency at the bifurcation, so $Z_d(\omega) = 1/\sqrt{\omega - \omega_H}$.

Using these results and (2.18), it is readily determined how the optimal $I(t)$ scales with ω when the desired spike time t_1 is a (fixed) small perturbation from the natural period $T = 2\pi/\omega$. Denoting by I_{max1} the maximum of $|I(t)|$ in this case, we get

$$I_{max1} = c_1\omega^2/Z_d(\omega) \tag{2.19}$$

for a fixed neuron model and time shift $t_1 - T$, to lowest order in $t_1 - T$. Here, c_1 is a model-dependent constant. In words, Eqn (2.19) shows how the amplitude of the optimal current required to perturb spike times by a fixed amount scales with the baseline frequency of the neuron. A complementary relationship is obtained by asking how this amplitude scales with baseline frequency when the optimal current perturbs the spike time by a fixed fraction of the (varying) baseline period. In this case, setting $t_1 - T$ in (2.18) to pT, where p is the fixed fraction, gives

$$I_{max2} = c_2\omega/Z_d(\omega). \tag{2.20}$$

For phase reductions near the SNIPER bifurcation, and for other cases in which $Z_d(\omega)$ decreases as ω increases, both expressions (2.19) and (2.20) demonstrate that the optimal currents required to perturb spike times diminish rapidly in amplitude at lower baseline frequencies. We will return to this point below.

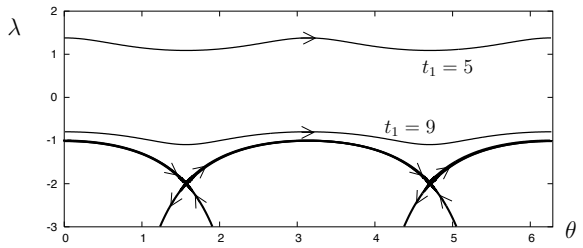

Figure 1. Phase space for (2.4) and (2.5) with the sinusoidal PRC (3.21) and $\omega = Z_d = 1$, and $\phi = 0$, showing fixed points at $(\theta,\lambda) = (\pi/2,-2)$ and $(3\pi/2,-2)$, stable and unstable manifolds of the fixed points, and trajectories with $t_1 = 5$ and $t_1 = 9$.

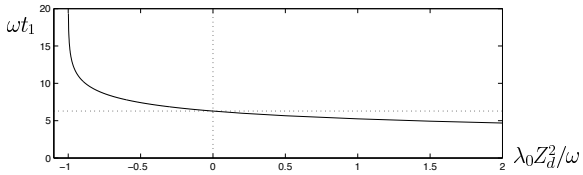

Figure 2. Dependence of t_1 on λ_0 for the sinusoidal PRC (3.21), as obtained from (3.22).

3 Examples

3.1 Sinusoidal PRC

Consider $f(\theta) = \omega =$ constant, corresponding to an intrinsically oscillatory neuron, and the PRC

$$Z(\theta) = Z_d \sin(\theta - \phi), \tag{3.21}$$

where Z_d and ϕ are constants. This might arise due to proximity to a supercritical Hopf or a Bautin bifurcation [4,10]. There are fixed points of the Euler-Lagrange equations (2.4) and (2.5) at $(\theta_f,\lambda_f) = (\pi/2+\phi,-2\omega/Z_d^2),(3\pi/2+\phi,-2\omega/Z_d^2)$, each with eigenvalues ω and $-\omega$. The phase space for (2.4) and (2.5) is shown in Figure 1 for $\omega = 1, Z_d = 1$, and $\phi = 0$.

For simplicity, in the following we take $\phi = 0$, which gives $Z(0) = 0$. We integrate (2.10) to give

$$t_1 = \frac{4}{\omega}K\left(-\frac{H_0 Z_d^2}{\omega^2}\right) = \frac{4}{\omega}K\left(-\frac{\lambda_0 Z_d^2}{\omega}\right). \tag{3.22}$$

Here $K(x)$ is the complete elliptic function of the first kind, a monotonically increasing function with properties that

$$K(0) = \pi/2, \qquad \lim_{x\to-\infty} K(x) = 0, \qquad \lim_{x\to 1} K(x) = \infty. \tag{3.23}$$

Figure 2 shows how t_1 depends on λ_0; as expected from (2.11), it decreases monotonically as λ_0 increases. Furthermore, as expected from Section 2.3, the initial condition $\lambda_0 = 0$ gives $t_1 = 2\pi/\omega$. Finally, from (3.22) and (3.23), we see that t_1 blows up to infinity as $H_0 \to -\omega^2/Z_d^2$; this is expected from Eqn. (2.10), as $-\omega^2/Z_d^2 = \sup_\theta\left(-[f(\theta)]^2/[Z(\theta)]^2\right)$. Recalling (2.12), this corresponds to approach toward the stable and unstable manifolds of the fixed points. This forces the trajectory to spend asymptotically long times near the fixed points, delaying its arrival to $\theta = 2\pi$.

To obtain the initial condition λ_0 for a particular value of t_1, one can in principle invert the function $K(x)$ in (3.22). In practice, it is easier to solve (2.4), (2.5) subject to the conditions $\theta(0) = 0, \theta(t_1) = 2\pi$ numerically using a shooting method. We used such a method to generate the optimal currents for $\omega = 1$, $Z_d = 1$, and $\phi = 0$ for various values of t_1 shown in Figure 3, where the time axis has been scaled for ease of comparison. Not surprisingly, if we want the neuron to fire more quickly than it would in the absence of the stimulus (i.e., if $t_1 < T$), the optimal current is positive (resp., negative) for θ values for which $Z(\theta)$ is positive (resp., negative). Furthermore, it is clear that the approximation (2.17) characterizes optimal currents for $t_1 \approx T$ (Fig. 4 (a)), and that the optimal current scales as expected with ω (Figure 5 (a)).

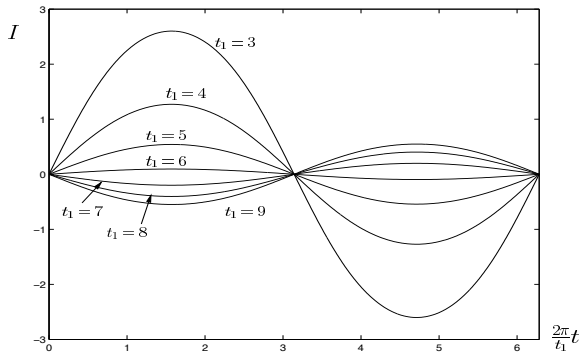

Figure 3. Optimal currents for the sinusoidal PRC (3.21) with $\omega = Z_d = 1$ and $\phi = 0$ for different values of t_1. The time axis has been scaled for ease of comparison.

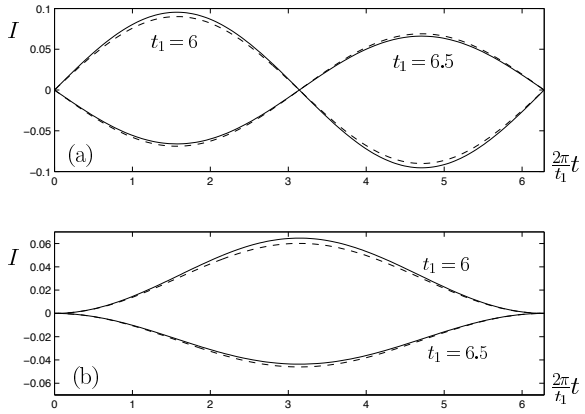

Figure 4. Exact (solid lines) and approximate (dashed lines) optimal currents for t_1 as labelled with (a) the sinusoidal PRC (3.21) with $\omega = Z_d = 1$ and $\phi = 0$, (b) the SNIPER PRC (3.24) with $\omega = Z_d = 1$, and (c) the PRC corresponding to the Hodgkin-Huxley equations with $I_b = 10$.

3.2 SNIPER PRC

Consider $f(\theta) = \omega = \text{constant}$, and the PRC

$$Z(\theta) = Z_d(1 - \cos\theta). \tag{3.24}$$

This could arise for neurons near a SNIPER bifurcation (i.e., a saddle-node bifurcation on a periodic orbit) [4,8]. Here, there is one fixed point of the Euler-Lagrange equations (2.4) and (2.5) at $(\theta_f, \lambda_f) = (\pi, -\omega/(2Z_d^2))$, with eigenvalues $\pm\omega/\sqrt{2}$. The phase space for (2.4) and (2.5) for this PRC is shown in Figure 6 for $\omega = 1$ and $Z_d = 1$. We again used a shooting method to find the optimal currents – a comparison for various values of t_1 is given in Figure 7. Again, (2.17) is a good approximation for $t_1 \approx T$ (see Figure 4(b)), and the expected scaling of optimal currents

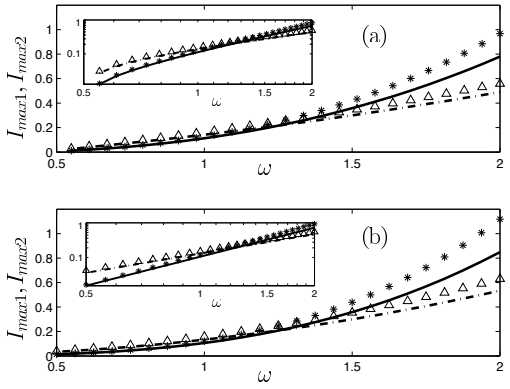

Figure 5. Scaling of the amplitude of optimal currents with baseline frequency ω, for (a) the sinusoidal PRC $Z(\theta) = \frac{1}{\sqrt{\omega - \omega_H}}\sin(\theta)$, with $\omega_H = 0.5$ and (b) the SNIPER PRC $Z(\theta) = \frac{1}{\omega}(1 - \cos(\theta))$. For $t_1 - T = -0.5$, the amplitude I_{max1} from the lowest-order expression Eqn. (2.19) is given by solid lines; stars give the analogous numerically computed values (i.e. to all orders). For the faction $p = 0.9$, the amplitude I_{max2} from the lowest-order expression Eqn. (2.20) is given by dot-dashed lines; triangles give the analogous numerical values. Insets give the same data on log-log axes.

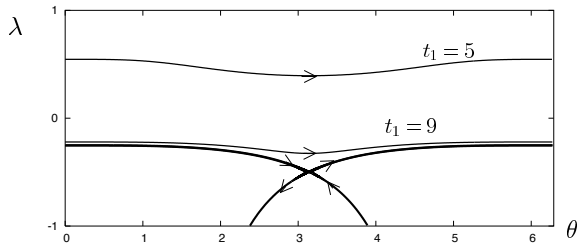

Figure 6. Phase space for (2.4) and (2.5) for the SNIPER PRC (3.24) with $\omega = 1$ and $Z_d = 1$, showing the fixed point at $(\theta, \lambda) = (\pi, -1/2)$, stable and unstable manifolds of the fixed point, and trajectories for periodic orbits with period $t_1 = 5$ and $t_1 = 9$.

with ω is seen (Figure 5 (b)).

3.3 Theta Neuron

The 'theta neuron' model describes both superthreshold and subthreshold dynamics near a SNIPER bifurcation [8]. With our control current $I(t)$, this model is

$$\frac{d\theta}{dt} = 1 + \cos\theta + (1 - \cos\theta)\,(I(t) + I_b)\,, \tag{3.25}$$

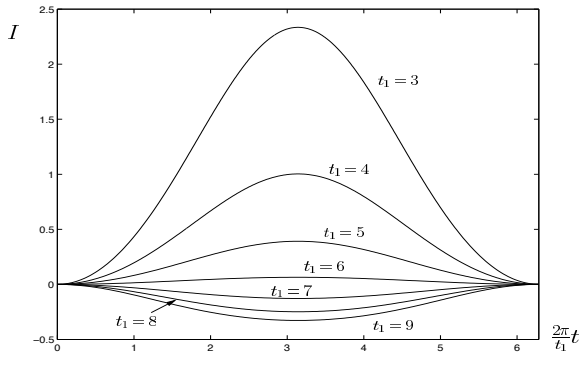

Figure 7. Optimal currents for the SNIPER PRC (3.24) with $\omega = Z_d = 1$ for different values of t_1. The time axis has been scaled for ease of comparison.

i.e., equation (2.1) with $f(\theta) = 1+\cos\theta + I_b(1-\cos\theta), Z(\theta) = 1-\cos\theta$. As above, θ is 2π-periodic and spikes are fired at $\theta = 0$. Here, I_b is the baseline current. If $I_b > 0$, the cell fires periodically in the absence of input $I(t)$, with angular frequency $2\sqrt{I_b}$. If $I_b < 0$, the model is excitable: no spikes will occur without input $I(t)$, as there are two fixed points (one of which is stable) for $I(t) = 0$; however, for appropriate inputs $I(t)$ spikes can occur.

When $I_b > 0$, applying the coordinate transformation $\theta(\phi) = 2\tan^{-1}\left(\sqrt{I_b}\tan(\phi/2-\pi/2)\right)+\pi$ to (3.25) gives $\frac{d\phi}{dt} = \omega + \frac{2}{\omega}(1-\cos\phi)I(t)$, which is identical to the governing equation for the SNIPER PRC with $Z_d = 2/\omega$. This transformation preserves $\theta(\phi = 0) = 0$ and $\theta(\phi = 2\pi) = 2\pi$, i.e., the property of spiking at 0 and 2π.

The Euler-Lagrange equations (2.4) and (2.5) for the theta neuron model have a fixed point at $(\theta_f, \lambda_f) = (\pi, -I_b)$, with eigenvalues $\pm\sqrt{2I_b}$. For $I_b < 0$, they also have fixed points at $(\theta_f, \lambda_f) = (\cos^{-1}((I_b+1)/(I_b-1)), 0)$, with eigenvalues $\pm 2\sqrt{-I_b}$. The phase space for the Euler-Lagrange equations for this model with $I_b = 0.25$ and $I_b = -0.25$ is shown in Figure 8. For large t_1 when $I_b < 0$, the solution spends most of its time near one of the two saddle points, with an increasingly punctate current pulse peaked halfway through its transit from $\theta = 0$ to $\theta = 2\pi$, as Fig. 9 shows.

3.4 Hodgkin-Huxley PRC

The Hodgkin-Huxley equations [16] are a system of four ODEs that model the generation of action potentials (i.e., spikes) in the squid giant axon, based on the dynamical interplay between ionic conductances and intracellular voltage. They have been highly influential, with most mathematical neuron models being based on them in one way or another.

Here we consider the Hodgkin-Huxley equations with standard parameters and applied baseline current $I_{HH} = 10$, for which the neuron fires periodically with period $T = 14.63$ ms, corresponding to $\omega = 0.4315$ rad/ms. The PRC for this system, computed numerically with XPP [9], is shown in Figure 10. To numerically study the Euler-Lagrange equations, we approximated the PRC obtained from XPP as a sum of terms in a Fourier series. It is found numerically that the Euler-Lagrange equa-

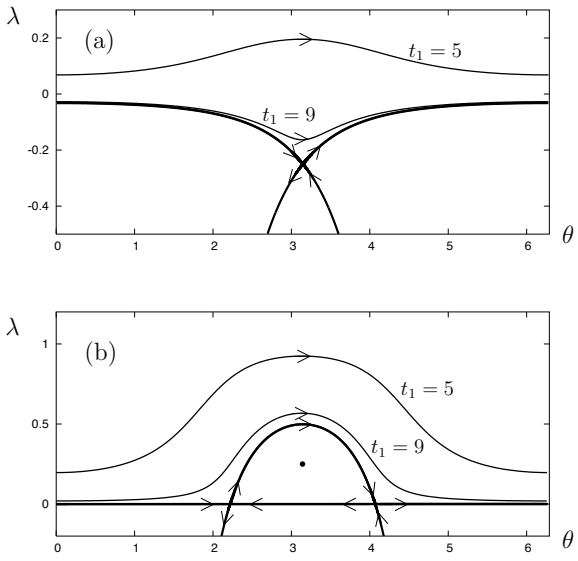

Figure 8. Phase space for (2.4) and (2.5) for the theta neuron model (3.25) with (a) $I_b = 0.25$, (b) $I_b = -0.25$, showing fixed points, stable and unstable manifolds of the fixed points, and trajectories for periodic orbits with period $t_1 = 5$ and $t_1 = 9$.

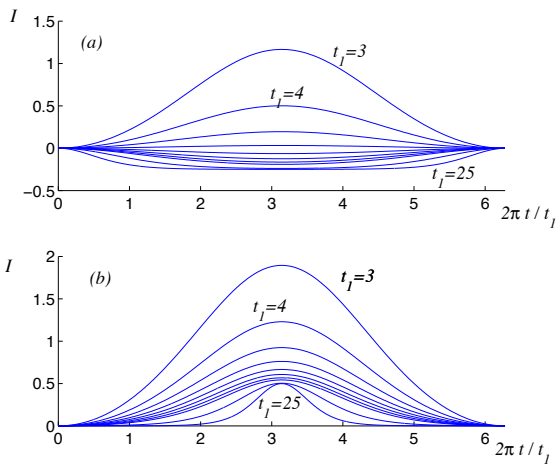

Figure 9. Optimal currents for the theta neuron model, (a) with $I_b = 0.25$ and (b) with $I_b = -0.25$, with time axis scaled as above. Target time values are, from top, $t_1 = 3, 4, 5, 6, 7, 8, 9, 10, 15, 25$.

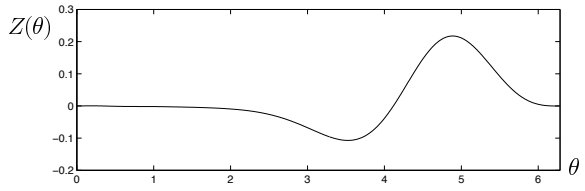

Figure 10. Phase response curve for the Hodgkin-Huxley equations with standard parameters and injected baseline current $I_{HH} = 10$.

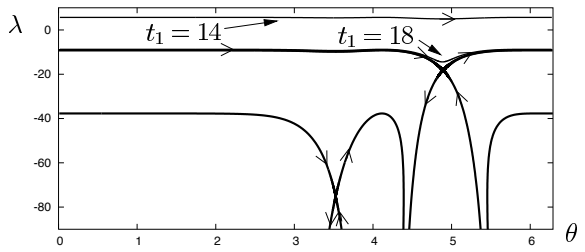

Figure 11. Phase space for (2.4) and (2.5) for the PRC corresponding to the Hodgkin-Huxley equations with $I_{HH} = 10$, showing the stable and unstable manifolds of the two fixed points, and trajectories for periodic orbits with period $t_1 = 14$ and $t_1 = 18$.

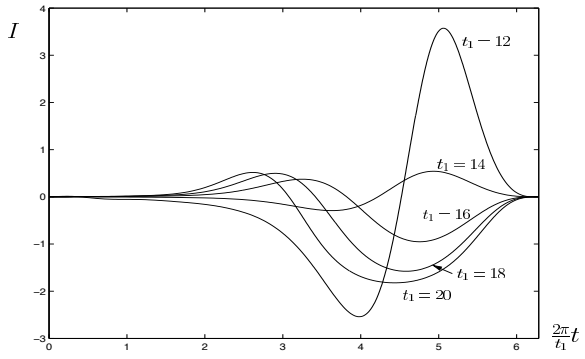

Figure 12. Optimal currents for the PRC for the Hodgkin-Huxley equations with standard parameters and with $I_{HH} = 10$ for different values of t_1. The time axis has been scaled for ease of comparison.

tions (2.4) and (2.5) for this PRC have fixed points at $(\theta, \lambda) = (3.53, -75.16)$ and $(4.89, -18.22)$, both saddles with eigenvalues approximately equal to ± 0.92. The phase space for (2.4) and (2.5) for this PRC is shown in Figure 11. We used a shooting method to find the optimal currents shown in Figure 12 for various values of t_1.

It is natural to ask to what extent the optimal current found using the phase model with this Hodgkin-Huxley PRC causes a neuron described by the *full* equations to fire at the specified

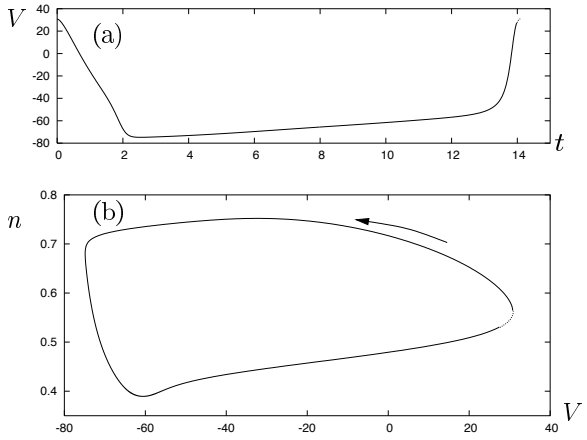

Figure 13. Dynamics of the full Hodgkin-Huxley equations with $I(t)$ chosen to be the optimal current stimulus for $t_1 = 14$ for the phase model with the Hodgkin-Huxley PRC for $I_{HH} = 10$. (a) shows the time series of the transmembrane voltage V, and (b) shows the phase space projection onto the (V, n) plane, where V is the voltage and n is a gating variable (using the standard Hodgkin-Huxley notation). The solid line segment shows the dynamics while $I(t)$ is being applied up to time t_1. The dotted segment shows the dynamics after $I(t)$ is turned off until the neuron first fires.

time. To answer this, we take initial conditions for the Hodgkin-Huxley equations following a spike, apply the optimal $I(t)$ found from the phase model until the specified time t_1, then allow the full equations to evolve under their natural dynamics without injected current. We measure the firing time as the time of the first peak in the voltage above an appropriate threshold.

For t_1 close to the intrinsic period, the Hodgkin-Huxley equations with these inputs fire at approximately the specified times t_1: see Figure 13 for $t_1 = 14$. In this case, $|I(t)|$ remains relatively small, which is necessary for the phase model to accurately characterize the full Hodgkin-Huxley equations [4, 18]. As t_1 moves away from the natural period, the optimal current from the phase model causes the full equations to spike later than the target time, as $|I(t)|$ becomes relatively large and the phase reduction loses validity. In fact, simulations show that this $I(t)$ pushes the trajectory near an unstable fixed point (not captured by the phase model) having complex eigenvalues with small, positive real parts. The time required for the trajectory to spiral away from this fixed point accounts for some of the discrepancy with the phase model. Figure 14 compares the specified time of firing t_1 and the actual time of firing t_1^{HH} for the full Hodgkin-Huxley equations, using the current found from optimizing the phase model.

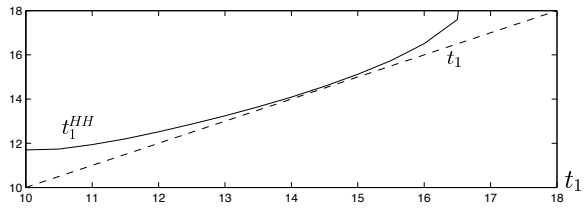

Figure 14. Comparison of the specificed time of firing t_1 and the actual time of firing t_1^{HH} for the full Hodgkin-Huxley equations for the current found from optimizing the phase model. The dashed line corresponds to exact agreement.

4 Optimal Current for Minimizing the Time of Firing

The previous sections were concerned with determining the optimal current to cause a neuron described by a phase model to fire at a specified time. Here, we consider optimizing the current, subject to the constraint that $|I(t)| \leq \bar{I}$ for all t, which causes the neuron described by a phase model to fire as quickly as possible. This constraint could represent the maximal possible synaptic input that upstream neurons can provide to the neuron at hand. Here, we do not constrain the rate with which $I(t)$ can vary; in practice, the timescale of the synaptic currents, which varies among synapse types but can be very rapid, determines the viability of this assumption of unconstrained rate.

The following argument suggests using 'bang-bang control,' in which the injected current takes the extreme values of $\pm\bar{I}$ [6]. From (2.1), in a time step dt the phase advances by

$$d\theta = [f(\theta) + Z(\theta)I(t)]dt. \tag{4.26}$$

To get the neuron to fire as quickly as possible, we maximize $d\theta$ at each timestep. Clearly, to do this we should take

$$I(t) = I^{bb}(\theta(t)) = \begin{cases} \bar{I} & \text{for } Z(\theta(t)) > 0 \\ -\bar{I} & \text{for } Z(\theta(t)) < 0 \end{cases}. \tag{4.27}$$

More completely, suppose that the neuron starts with initial phase θ_i. It will fire at time t_f given by

$$t_f = \int_0^{t_f} dt = \int_{\theta_i}^{2\pi} \frac{d\theta}{f(\theta) + Z(\theta)I(t)}, \tag{4.28}$$

where we assume that $f(\theta) + Z(\theta)I(t)$ is always positive (if not, then from (4.26) the phase does not advance). Now, if $-|Z(\theta)|\bar{I} < Z(\theta)I(t) < |Z(\theta)|\bar{I}$, that is, the current $I(t)$ satifies the amplitude constraint and is not given by (4.27),

$$\frac{1}{f(\theta) + Z(\theta)I(t)} > \frac{1}{f(\theta) + |Z(\theta)|\bar{I}} > 0. \tag{4.29}$$

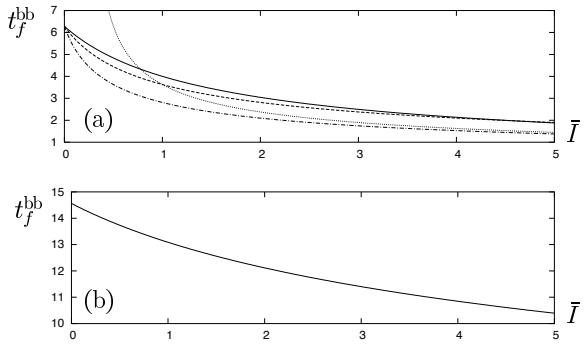

Figure 15. Minimal time of firing t_f^{bb} as a function of $\bar{I}$, obtained using bang-bang control, for phase models starting at $\theta_i = 0$ for (a) solid line: $f(\theta) = \omega = 1, Z(\theta) = \sin\theta$; dashed line: $f(\theta) = \omega = 1, Z(\theta) = 1 - \cos\theta$; dot-dashed line: the theta neuron model with $I_b = 0.25$; dotted line: the theta neuron model with $I_b = -0.25$, and (b) the PRC for the Hodgkin-Huxley equations with standard parameters and $I_b = 10$.

Then,

$$t_f = \int_{\theta_i}^{2\pi} \frac{d\theta}{f(\theta) + Z(\theta)I(t)} > \int_{\theta_i}^{2\pi} \frac{d\theta}{f(\theta) + |Z(\theta)|I^{bb}(\theta)} \equiv t_f^{bb}, \tag{4.30}$$

where t_f^{bb} is the time the neuron fires for the injected current given by (4.27). Note that for bang-bang control to work, it is necessary that $f(\theta) + |Z(\theta)|\bar{I} > 0$ for all θ. Figure 15 shows t_f^{bb} for $\theta_i = 0$ for the PRCs considered in the previous section. For all except the theta neuron model with negative I_b, for which one needs $\bar{I} > -I_b$ in order for bang-bang control to produce a spike, we see that t_f^{bb} approaches the natural period as $\bar{I} \to 0$, as expected.

5 Discussion and conclusion

In this paper, we first show that there is a unique optimal current $I(t)$ that will elicit a spike at a specified time t_1 for phase-reduced neural models satisfying a general set of conditions. We then derive additional results about this current $I(t)$ for intrinsically oscillatory models, using the formalism of PRCs. In particular, for these models we show that the time course of the optimal current will be proportional to the PRC itself for small perturbations in spike times. This fact, coupled with earlier results about the typical scaling of PRCs, enables us to study how the amplitude of this current scales with the baseline (i.e., unperturbed) frequency of the oscillatory model. Finally, we discuss bang-bang control, computing the earliest spike times that can be elicited in different neural models by currents of fixed maximal amplitude. All of these results are illustrated with phase-reduced neural models valid near the SNIPER and Hopf bifurcations, and

with a numerically derived phase model for the Hodgkin-Huxley equations.

Our results on the form and scaling of optimal currents $I(t)$ address the question of how the dynamics of individual neurons determine the processing of synaptic inputs to produce spikes. Specifically, they imply that the standard classification of a neuron's PRC as Type I vs Type II [8] depending, respectively, on whether it is nonnegative (as for the SNIPER PRC) or takes both positive and negative values (as for the sinusiodal PRC), also determines, respectively, whether purely excitatory synapses or a mixture of excitatory and inhibitory synapses are required to optimally adjust its spike times. As previous work [4,8,10] shows that PRCs remain invariant in form but typically increase in amplitude as baseline oscillation frequencies decrease, we also conclude that the optimal inputs for a given neuron operating at different frequencies are determined by rescaling in both time and amplitude a *single* curve of a given form. For the standard neural models studied here, the amplitude of the current that optimally causes a fixed perturbation in spike times decreases rapidly with the model's baseline frequency, indicating increased sensitivity at low firing rates. This type of increased sensitivity, or *gain*, at lower firing rates has been emphasized in the context of population-averaged firing rates in [4,15], and is extended here to the spike times of individual neurons.

In the context of many of the neural inputs that occur in vivo, the present results may nonetheless be viewed as rather limited, as many neurons receive inputs from up to thousands of afferent synapses and the combined currents contain components distinct from the optimal inputs considered here. One approach to this more general problem is to compute time-dependent components, or 'features,' of neural inputs whose combined strengths determine whether or not a given input will elicit a spike (see [19] and references therein). In particular, [1] shows that only a few such components are required to make this determination to quite high accuracy for the Hudgkin-Huxley (HH) equations. It will be interesting to investigate the relationship between this feature-based approach and that taken in the present paper, especially because the dominant such feature identified for the HH equations in [1] resembles in form the optimal currents for these equations computed here.

We close by mentioning an alternative approach to the problem of complex neural inputs to the probabilistic approach taken in [1,19]: exploring the entire family of inputs $I(t)$ that elicit a spike at time t_1. The complement to this 'level set' of inputs would then correspond to the (span of the) dominant features identified in [1,19]. This level set based approach was developed to answer related questions for other physical models in [20], and we have checked that the formalism extends readily to phase-reduced neuron models. As such, the optimal inputs studied in this paper may be viewed as distinguished points on the level set from which to begin this future analysis.

Acknowledgments
J. M. was supported by an Alfred P. Sloan Research Fellowship in Mathematics, E. S.-B. was supported by a National Sciences Foundation Postdoctoral Research Fellowship, and H.R. acknowledges support from the National Science Foundation. We thank X.J. Feng and Eduardo Sontag for helpful discussions.

REFERENCES

[1] B. Aguera y Arcas, A. Fairhall, and W. Bialek. Computation in a single neuron: Hodgkin and Huxley revisited. *Neural Comp.*, 15:17151749, 2003.

[2] P. Ashwin and J. Swift. The dynamics of N weakly coupled identical oscillators. *J. Nonlin. Sci.*, 2:69–108, 1992.

[3] E. Brown, P. Holmes, and J. Moehlis. Globally coupled oscillator networks. In E. Kaplan, J.E. Marsden, and K.R. Sreenivasan, editors, *Problems and Perspectives in Nonlinear Science: A celebratory volume in honor of Lawrence Sirovich*, pages 183–215. Springer, New York, 2003.

[4] E. Brown, J. Moehlis, and P. Holmes. On the phase reduction and response dynamics of neural oscillator populations. *Neural Comp.*, 16:673–715, 2004.

[5] E. Brown, J. Moehlis, P. Holmes, E. Clayton, J. Rajkowski, and G. Aston-Jones. The influence of spike rate and stimulus duration on noradrenergic neurons. *J. Comp. Neuroscience*, 17:13–29, 2004.

[6] A. Bryson and Y. Ho. *Applied Optimal Control*. Washington, D.C., Halsted Press, 1975.

[7] A. Cohen, P. Holmes, and R.H. Rand. The nature of coupling between segmental oscillators of the lamprey spinal generator for locomotion: a model. *J. Math Biol.*, 13:345–369, 1982.

[8] G. B. Ermentrout. Type I membranes, phase resetting curves, and synchrony. *Neural Comp.*, 8:979–1001, 1996.

[9] G. B. Ermentrout. *Simulating, Analyzing, and Animating Dynamical Systems: A Guide to XPPAUT for Researchers and Students*. SIAM, Philadelphia, 2002.

[10] G.B. Ermentrout and N. Kopell. Frequency plateaus in a chain of weakly coupled oscillators, I. *SIAM J. Math. Anal.*, 15:215–237, 1984.

[11] D. B. Forger and D. Paydarfar. Starting, stopping, and resetting biological oscillators: in search of optimal perturbations. *J. theor. Biol.*, 230:521–532, 2004.

[12] W. Gerstner, L. van Hemmen, and J. Cowan. What matters in neuronal locking? *Neural Comp.*, 8:1653–1676, 1996.

[13] R. M. Ghigliazza and P. Holmes. A minimal model of a central pattern generator and motoneurons for insect locomotion. *SIAM J. on Applied Dynamical Systems*, 3(4):671–700, 2004.

[14] D. Hansel, G. Mato, and C. Meunier. Phase dynamics for weakly coupled Hodgkin-Huxley neurons. *Europhys. Lett.*, 25(5):367–372, 1993.

[15] A. Herrmann and W. Gerstner. Noise and the PSTH responne to current transients: I. General theory and application to the integrate-and-fire neuron. *J. Comp. Neurosci.*, 11:135–151, 2001.

[16] A. L. Hodgkin and A. F. Huxley. A quantitative description of membrane current and its application to conduction and excitation in nerve. *J. Physiol.*, 117:500–544, 1952.

[17] N. Kopell and G.B. Ermentrout. Phase transitions and other phenomena in chains of coupled oscillators. *SIAM J. Appl. Math.*, 50:1014–1052, 1990.

[18] Y. Kuramoto. Phase- and center-manifold reductions for large populations of coupled oscillators with application to non-locally coupled systems. *Int. J. Bif. Chaos*, 7:789–805, 1997.

[19] F. Rieke, D. Warland, R. de Ruyter van Steveninck, and W. Bialek. *Spikes: Exploring the Neural Code*. MIT Press, Cambridge, MA, 1996.

[20] A. Rothman, T-S. Ho, and H. Rabitz. Exploring level sets of quantum control landscapes. *Phys. Rev. A.* submitted.

[21] P. A. Tass. *Phase Resetting in Medicine and Biology*. Springer, New York, 1999.

[22] D. Taylor and P. Holmes. Simple models for excitable and oscillatory neural networks. *J. Math. Biol.*, 37:419–446, 1998.

[23] H. Tuckwell and J. Feng. Optimal control of neuronal activity. *Phys. Rev. Lett.*, 91:018101–1 – 018101–4, 2005.

[24] A. Winfree. *The Geometry of Biological Time, Second Edition*. Springer, New York, 2001.